Quark Initial State Interaction in Deep Inelastic Scattering and the Drell-Yan process [*]

O. Linnyk[†], S. Leupold, U. Mosel

Institut für Theoretische Physik, Universität Giessen, Germany
February 2, 2008

Abstract

We pursue a phenomenological study of higher twist effects in high energy processes by taking into account the off-shellness (virtuality) of partons bound in the nucleon. The effect of parton off-shellness in deep inelastic $ep \rightarrow eX$ scattering (DIS) and the Drell-Yan process ($pp \rightarrow l\bar{l}X$) is examined. Assuming factorization and a single-parameter Breit-Wigner form for the parton spectral function, we develop a model to calculate the corresponding off-shell cross sections. Allowing for a finite parton width ≈ 100 MeV, we reproduce the data of both DIS and the triple differential Drell-Yan cross section without an additional K-factor. The results are compared to those from perturbative QCD and the intrinsic-k_T approach.

1 Introduction

One of the major goals of present day research is to study the structure of the nucleon and other hadrons in terms of the fundamental quark-gluon dynamics. In high energy hadronic processes like DIS, the Drell-Yan process, jet production, *etc.,* the soft and hard subprocesses can be disentangled. The hard cross section can be calculated using the well established methods of perturbative QCD. This procedure allows one to extract the information about the nonperturbative quark and gluon properties in a bound state from the experimental data.

[†]olena.linnyk@theo.physik.uni-giessen.de

The described method, based on factorization, is analogous to the Plane Wave Impulse Approximation (PWIA) for the description of quasi-elastic $(e, e'p)$ scattering in nuclear physics. The approximation of quasi-free constituents is valid when the binding energy is small compared to the energy transfered. In the theory of nuclei, the effects beyond the PWIA (such as photon radiation, initial state interaction (ISI) and final state interaction) are known to be essential for understanding semi-exclusive observables. Measurements, in which energy and momentum of the nucleon can be determined from the final state kinematics, offer an opportunity to study these effects and thus probe the nucleon interaction in nuclei [1, 2]. One would like to gain an understanding of the hadron structure which is as good as the present understanding of the compositeness of the nucleus in terms of nucleons and their interaction.

In the present paper, deep inelastic scattering and the Drell-Yan pair production are considered. Our aim is to investigate a kinematical region where standard perturbative QCD no longer works and where we thus need to model nonperturbative effects. Higher twists, suppressed by inverse powers of the hard scale Q^2, are important in description of low x_{Bj} DIS [3], hadron-hadron collisions [4], and semi-inclusive DIS at moderate energies [5]. In the case of fully inclusive DIS, the factorization of higher twist contribution in terms of a hard coefficient and the matrix element of quark and gluon fields in the nucleon was proven [4]. Coefficients of the twist expansion were calculated in [6]. But the matrix element is a non-perturbative object and has to be modelled. In the present work we model the power corrections by dressing the active parton lines with spectral functions. Figure 1 shows a handbag graph with the relevant initial state interactions which could build up a finite parton width.

The initial and final state parton interaction effects on the observable hard scattering cross sections have recently attracted a lot of attention. The essential role of final state interactions in the interpretation of the measured DIS structure functions at finite Q^2 has been stressed in [3, 7, 8]. In several other calculations [9, 10, 11, 12, 13, 14], non-collinear kinematics, *i.e.,* non-vanishing primordial transverse momenta of the partons in the nucleon, was considered. The authors of [15, 16] pointed out that one gluon exchange in the initial state can produce a large effect in πp scattering in the framework of a quark-diquark model. On the other hand, parton off-shellness effects in DIS and the Drell-Yan process can have the same order of magnitude as those of the intrinsic transverse momentum [17]. Thus, a consistent treatment of both is necessary to go beyond the PWIA in these reactions. In this paper, we develop the formalism to study these effects and apply it to calculate the cross sections of DIS and the Drell-Yan process.
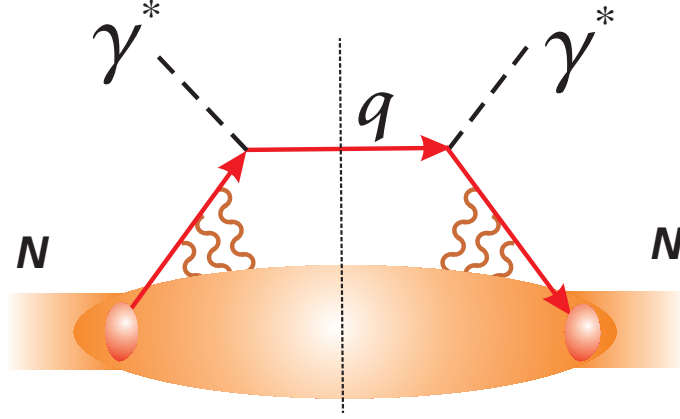
Figure 1: The handbag graph for DIS and the relevant initial state interactions that could build up a finite parton width.

Since the triple differential Drell-Yan cross section is a more exclusive observable than the DIS cross section, it is expected to be more sensitive to the ISI. The results of our calculations confirm this intuitive expectation. By taking into account both the finite width generated by ISI and the non-collinearity of partons, we reproduce the experimentally measured fully inclusive DIS cross section and the triple-differential cross section of the Drell-Yan process very well. Our success in reproducing the transverse momentum distribution of the Drell-Yan lepton pairs is particularly interesting, since other models disagree with experiment. In leading order of perturbative QCD, a delta function at zero transverse momentum is predicted. Only after the resummation of all orders in α_S, the pQCD predictions for the Drell-Yan pair p_T-distributions are reliable [18, 19, 20]. Among the next-to-leading order contributions to the dilepton cross section, only the gluon Compton scattering can give non-vanishing transverse momentum (p_T). This process, however, contributes only in the region of very high p_T: $p_T \geq \sqrt{M}$, where M is the mass of Drell-Yan pair. In contrast, the major part of the measured pairs lies in the interval $0 < p_T < \sqrt{M}$ and is not described by leading twist perturbative QCD [21]. At the same time, none of the phenomenological models, including intrinsic k_T approach, is able to reproduce simultaneously magnitude and shape of the experimentally observed distribution. In contrast, as we will demonstrate below, the data can be successfully described by a model which allows for off-shell partons.

The applied technique is presented in section 2 and the obtained results are discussed in section 3, followed by a short summary. We discuss the

interesting question of the application of factorization to hadron scattering in the Target Rest Frame in the Appendix.

2 Method

The basic tool in the calculation of hard processes is the factorization into hard and soft physics:

$$d\sigma = \sum_i e_i^2 f_i(\xi, \vec{p}_\perp) \otimes d\hat{\sigma}(\xi, \vec{p}_\perp), \tag{1}$$

where the sum runs over all relevant parton flavors, e_i is the charge of the ith type of parton in units of the proton charge e. $d\hat{\sigma}$ is the elementary cross section for a given process, $f(\xi, \vec{p}_\perp)$ are unintegrated parton distributions defined as [22]:

$$f(\xi, \vec{p}_\perp) = \frac{1}{4\pi} \int d^4y \ \langle N|\bar{\psi}(y)\gamma^+\psi(0)|N\rangle \ e^{ip\cdot y}\delta(y^+), \tag{2}$$

where $\xi \equiv p^+/P^+$ is the Nachtmann variable and p and P are momenta of the active parton and hadron, respectively. In [31], the factorization in the form (1) was proven in the leading power of the hard scale (photons virtuality in DIS and the Drell-Yan process).

Note that the unintegrated distributions do not depend on p^- due to $\delta(y^+)$. In other words, the parton distributions measure the correlation of partons with equal light cone times ($y^+ = 0$). This reflects the fact that the structure functions, measured in the fully inclusive DIS, depend only on P^+ in the Bjorken limit. To see this, let us consider the hadron tensor measured in DIS [23]:

$$W_{\mu\nu}(q) = \frac{1}{4\pi} \int d^4y e^{iq\cdot y}\langle N|J_\mu(y)J_\nu(0)|N\rangle_c. \tag{3}$$

In the hadron rest frame (M_N is the nucleon mass) :

$$(q_+, q_-, \vec{q}_T) = \left(-M_N x_{Bj}, \frac{Q^2}{M_N x_{Bj}}, \vec{0}\right), \tag{4}$$

As $Q^2 \to \infty$ with $x_{Bj} \equiv Q^2/P{\cdot}q$ finite and fixed, $q_- \to \infty$. As a consequence, the integral in (3) should vanish due to the fast oscillating exponent, unless

$$y_+ \to 0. \tag{5}$$

At the same time, y_- is finite and even large y_- can contribute to $W_{\mu\nu}$ in some cases. To be precise, the restriction on y_- is [23] :

$$|y_-| < 1/(M_N x_{Bj}). \tag{6}$$

In case of a fully inclusive process, one has the following condition due to causality:

$$y^2 = y_- y_+ - \vec{y}_T^2 \geq 0 \implies \vec{y}_T \to \vec{0}. \tag{7}$$

Thus, DIS in the Bjorken limit is a light-cone ($y^2 \to 0$) dominated process and the hadronic part of the DIS cross section is a function of a single variable $p^+ \equiv x_{Bj} P^+$.

The factorization formula (1) is valid only in the scaling limit, *i.e.*, at the leading power as $Q^2 \to \infty$. On the other hand, at moderate Q^2 considerable p^--dependent corrections might be necessary to make predictions for semi-exclusive observables, *e.g.* Drell-Yan lepton pair production cross section and asymmetries. In this case, we propose the following factorization ansatz:

$$d\sigma = \sum_i e_i^2 g_i(\xi, \vec{p}_\perp, p^-) \otimes d\hat{\sigma}(\xi, \vec{p}_\perp, p^-). \tag{8}$$

The difference between (1) and (8) is precisely due to off-shellness effects that we aim to study. Indeed, the minus component of the free parton momentum is fixed by the on-shell condition:

$$p^2 = p^+ p^- - \vec{p}_\perp^2 = \xi P^+ p^- - \vec{p}_\perp^2 = 0 \tag{9}$$

(we put the current quark mass to zero). However, since the partons are bound in the nucleon, (9) no longer holds. Thus all the 4 components of the parton momentum are independent and the full propagator should be used. In this case, the cross section is calculated using a virtuality distribution defined by a parton spectral function [24, 25]. Spectral functions of quarks in quark matter are, for example, calculated in [26].

In nuclear physics, the terms off-shellness and virtuality are often interchanged. The on-shell condition for the nucleon reads $P^2 = M_N^2$, where M_N is the nucleon mass in vacuum. Thus, only 3 components of the on-shell nucleon's 4-momentum are independent. In case of an interacting nucleon, P^2 is no longer fixed and its distribution (spectral function) is given by the details of the interaction. All four components of the off-shell nucleon's momentum are independent. Thus, a hadron is said to be off-shell, if its momentum squared is different from the free hadron mass, *i.e.* when it is virtual.

Partons in the nucleon are always virtual. For example, in the naive parton model, the parton momentum squared is $p^2 = (x_{Bj}P)^2 = x_{Bj}^2 M_N^2$, which is usually far from the current parton mass ($= 0$ in our calculations). We call a parton off-shell, if the parton's momentum has four independent components. In this case the parton off-shellness p^2 is not fixed and should be integrated over. This differs from the "trivial off-shellness" of parton model, in which the quark is virtual, but it's off-shellness is fixed (to $x_{Bj}^2 M_N^2$). More

realistically, one should include the transverse motion of partons. Then, for a free parton, $p^- = p_\perp^2/p^+$. In our calculations, p^- is not fixed by p^+ and $p_\perp^2$. Instead, we integrate over all kinematically allowed p^-.

In the following, we additionally assume that the dependence of g on p^- factorizes from the $p_\perp$-dependence:

$$d\sigma = \sum_i e_i^2 \tilde{f}_i(\xi, \vec{p}_\perp) \otimes d\hat{\sigma}(\xi, \vec{p}_\perp, m) \otimes A(m, \Gamma). \qquad (10)$$

In (10), $d\hat{\sigma}(\xi, \vec{p}_\perp, m)$ is the off-shell partonic cross section and $m \equiv \sqrt{p^2}$ the parton's off-shellness. We choose

$$\tilde{f}_i(\xi, \vec{p}_\perp) = f_i(\xi, \vec{p}_\perp). \qquad (11)$$

Identifying $\tilde{f}_i(\xi, p_\perp)$ with the usual parton distribution functions means that we apply a quasiparticle picture, in which all effects involving more than one parton are encoded in the spectral function. The latter includes a width caused by parton-parton interactions (see *e.g.* [26] and references therein).

In our calculations, a Breit-Wigner parametrization for the parton spectral function $A(m, \Gamma)$ was applied:

$$A(m, \Gamma) = \frac{1}{\pi} \frac{\Gamma}{m^2 + \frac{1}{4}\Gamma^2}. \qquad (12)$$

The width Γ of partons was considered constant. We find its value by comparing the calculated cross section to the data. Note that for simplicity we use the same $A(m)$ for all parton types.

The hard part, *i.e.,* the partonic cross section, is calculated using the rules of perturbative Quantum Chromodynamics (pQCD). We calculated the pQCD differential cross section for an electron scattering off a virtual quark and that for the annihilation of an off-shell quark-antiquark pair into a pair of dileptons (see (37) below). Both off-shell partonic cross sections turned out to be gauge invariant due to the on-shell leptons making the modification of the vertex by Ward's identity unnecessary.

The analysis of the off-shell kinematics and the obtained cross sections are separately given below for DIS and the Drell-Yan process. The case of electron scattering (section 2.1) is simpler and serves as an introduction to the calculation of the Drell-Yan pair transverse momentum distribution in section 2.2.

6

2.1 DIS

Ignoring the off-shellness of partons, the factorization formula (1) for DIS can be written as:

$$\frac{d\sigma}{d\hat{t}d\hat{u}} = \sum_i e_i^2 \int_0^1 d\xi \int d\vec{p}_\perp f_i(\xi, p_\perp)\frac{d\hat{\sigma}}{d\hat{t}d\hat{u}}, \tag{13}$$

$$\left(\frac{d\hat{\sigma}}{d\hat{t}d\hat{u}}\right)_{\text{on-shell}} = \frac{2\pi\alpha^2}{\hat{t}^2\hat{s}^2}\left(\hat{s}^2 + \hat{u}^2\right)\delta(\hat{s} + \hat{u} + \hat{t}), \tag{14}$$

where s, t, u are the Mandelstam variables, $\alpha = e^2/4\pi$, the parton quantities are labeled with hats, and the δ-function reflects the on-shell condition on the parton level:

$$\hat{s} + \hat{u} + \hat{t} = 0. \tag{15}$$

Let us consider the Bjorken limit ($Q^2 \to \infty$ with x_{Bj} -fixed, where q is the momentum transfer, $Q^2 \equiv -q^2$) in the rest frame of the nucleon. In this limit, the partonic and hadronic invariants are simply related:

$$\hat{t} = t, \quad \hat{s} = \xi s, \quad \hat{u} = \xi u. \tag{16}$$

From (15) and (16) one gets the constraint

$$\xi \to -\frac{t}{s+u} = -\frac{q^2}{2P \cdot q} \equiv x_{Bj}. \tag{17}$$

The parton model cross section of DIS is obtained:

$$\left(\frac{d\sigma}{dtdu}\right)_{\text{LO}} = \sum_i e_i^2 x_{Bj} f_i(x_{Bj})\left(\frac{2\pi\alpha^2}{t^2 s^2}\frac{(s^2 + u^2)}{s+u}\right), \tag{18}$$

where

$$f_i(x_{Bj}) \equiv \int dp_\perp f_i(x_{Bj}, p_\perp),$$

"LO" stands for leading order of perturbative QCD, *i.e.* parton model.

For finite Q^2, the fact that the partons are off-shell can generate large corrections to the formulas (15)-(18). We would like to point out the important analogies and differences to the on-shell case:

- The energy-momentum conservation reads (*c.f.* (15))

$$\hat{s} + \hat{u} + \hat{t} = m^2, \tag{19}$$

where $m^2 \equiv p^2$ denotes the virtuality of the struck parton.

- In case of an off-shell initial quark, we find the following relation between the partonic and hadronic variables

$$\hat{t} = t = -Q^2, \quad \hat{s} = \xi(s - M_N^2) + m^2,$$

$$\hat{u} = Q^2 - \xi(s - M_N^2) = \xi(u + M_N^2) + Q^2(1 - \frac{\xi}{x_{Bj}}), \quad (20)$$

which coincides with (16) in the Bjorken limit. We choose the z-axis along the incoming electron.

- The hadron light cone momentum fraction carried by the struck parton ($\xi \equiv p^+/P^+$) is not equal to the Bjorken x_{Bj}, unless $Q^2 \to \infty$. The relation between x_{Bj} and ξ is

$$x_{Bj} = \xi \frac{Q^2}{Q^2 - m^2 - \xi(M_N^2 - \frac{m^2 + \vec{p}_\perp^2}{\xi^2})\frac{Q^2}{s - M_N^2} + 2\vec{p}_\perp \vec{q}_\perp}. \quad (21)$$

Relation (21) yields a nonlinear equation for x_{Bj}, because $\vec{q}_\perp$ depends on x_{Bj} as follows:

$$\vec{q}_\perp^2 = Q^2(1 - \frac{Q^2}{s - M_N^2}(\frac{1}{2x_{Bj}} + \frac{M_N^2}{s - M_N^2})). \quad (22)$$

One can see that $\vec{q}_\perp^{\,2} \leq Q^2$ and that it reaches its maximum at $s \gg Q^2/2x$. Due to (21), the ISI in DIS can be interpreted as a smearing of the parton momentum fraction ξ around its parton model value x_{Bj}. In the following three cases equation (21) simplifies:

- Taking the Bjorken limit:

$$x_{Bj} = \xi. \quad (23)$$

- Neglecting the transverse momentum of the struck parton inside the nucleon, but keeping $m^2 \neq 0$:

$$x_{Bj} = \xi \frac{Q^2}{Q^2 - m^2 - \xi(M_N^2 - \frac{m^2}{\xi^2})\frac{Q^2}{s - M_N^2}}. \quad (24)$$

- Taking into account both the parton's transverse momentum and off-shellness, but considering the limit $s \gg Q^2/2x$, $s \gg M_N^2$:

$$x_{Bj} = \xi \frac{Q^2}{Q^2 - m^2 + 2|\vec{p}_\perp|\sqrt{Q^2}\cos(\phi)}, \quad (25)$$

where ϕ is the azimuthal angle of the quark momentum. As Q^2 goes to infinity, equation (25) coincides with (23).

8

- The off-shell partonic cross section is

$$\left(\frac{d\hat{\sigma}}{d\hat{t}d\hat{u}}\right)_{\text{off-shell}} = \frac{2\pi\alpha^2}{\hat{t}^2\hat{s}^2}\left(\hat{s}^2 + \hat{u}^2\right)\delta(\hat{s} + \hat{u} + \hat{t} - m^2), \qquad (26)$$

where $\hat{u}$ and $\hat{s}$ depend on m^2 via (20) and (21).

Therefore, the leading order expression for the Lorentz invariant DIS cross section (18) is modified by the ISI as follows:

$$\left(\frac{d\sigma}{dtd\hat{u}}\right)_{\text{ISI}} = \sum_i e_i^2 \int\limits_0^\infty dm\, \text{A}(m,\Gamma) \int\limits_0^1 d\xi \int d\vec{p}_\perp\, f_i(\xi,\vec{p}_\perp) \left(\frac{d\sigma}{dtd\hat{u}}\right)_{\text{off-shell}} \qquad (27)$$

To compare to the experiment or to the leading order cross section (18), we also need to change variables from partonic $\hat{u}$ to hadronic u or x_{Bj} (x_{Bj} is related to the hadronic Mandelstam variables (s, t, u) by (17)). We choose the following independent variables for the hadronic cross section:

$$s,\ t,\ x_{Bj}. \qquad (28)$$

The partonic cross section depends on:

$$s,\ t,\ \hat{u},\ m^2,\ \xi,\ \vec{p}_\perp. \qquad (29)$$

We have related the partonic $\hat{s}$ to s by (20). The transformation from one set of variables to the other is done in the following way:

$$\left(\frac{d\sigma}{dtdx_{Bj}}\right)_{\text{ISI}} = \int d\hat{u} \left(\frac{d\sigma}{dtd\hat{u}}\right)_{\text{ISI}} \delta(x_{Bj} - x_{Bj}(s,t,\hat{u})), \qquad (30)$$

where $(d\sigma/dtd\hat{u})$ is given by (27) and x_{Bj} as a function of the variables (29) is defined by (21). We note in passing that $(d\sigma/dtdx_{Bj})$ is negative, while $(d\sigma/dtd\hat{u})$ is positive. This has to be taken into account in (30) by an appropriate choice of integration boundaries. From equations (26), (27), (30), we obtain:

$$\left(\frac{d\sigma}{dtdx_{Bj}}\right)_{\text{ISI}} = \sum_i \frac{2\pi\alpha^2 e_i^2}{t^2} \int\limits_0^\infty dm\, \text{A}(m,\Gamma) \int\limits_0^1 d\xi \int d\vec{p}_\perp\, f_i(\xi,\vec{p}_\perp) \int d\hat{u}$$
$$\frac{(\hat{s}^2 + \hat{u}^2)}{\hat{s}^2}\, \delta\left(\hat{s} + \hat{u} + t - m^2\right) \delta\left(x_{Bj} - x_{Bj}(s,t,\hat{u},\xi,m^2,\vec{p}_\perp)\right), (31)$$

9

where $\hat{s} = \xi(s - M_N^2) + m^2$. The integration over $\hat{u}$ can be done using one of the δ-functions. The result is:

$$\left(\frac{d\sigma}{dtdx_{Bj}}\right)_{\text{ISI}} = \sum_i \frac{2\pi\alpha e_i^2}{t^2} \int\limits_0^\infty dm\, A(m,\Gamma) \int\limits_0^1 d\xi \int d\vec{p}_\perp\, f_i(\xi, \vec{p}_\perp)$$
$$\times \left(1 + \frac{(Q^2 - \xi(s - M_N^2))^2}{(\xi(s - M_N^2) + m^2)^2}\right) \delta\left(x_{Bj} - x_{Bj}(s, t, \hat{u}, \xi, m^2, \vec{p}_\perp)\right), \quad (32)$$

where $x_{Bj}(s, t, \hat{u}, \xi, m^2, \vec{p}_\perp)$ is given by (21) and $\hat{u} = -t - \xi(s - M_N^2)$. The δ-function can be used to perform the integration over the azimuthal angle of the parton momentum. The remaining three integrations must be performed numerically. The limit $s \gg M_N^2, Q^2/2x$ was taken for simplicity. For the unintegrated parton distributions $f(\xi, \vec{p}_\perp)$ we use the factorized form (42) discussed in more detail in the next section. The results for DIS are presented in Sec. 3.1.

2.2 Drell-Yan process

We applied the same technique to calculate the cross section of the Drell-Yan process $(pp \rightarrow X + l^+l^-)$. In this case, an off-shell quark-antiquark pair annihilates into a pair of leptons. The virtuality of the quark (antiquark) coming from the target proton $(m_1^2 \equiv p_1^2)$ and that of the antiquark (quark) coming from the projectile proton $(m_2^2 \equiv p_2^2)$ are in general not equal. We assume, however, that their distributions $A(m)$ are the same.

The connection between the observables and partonic variables in case of two off-shell particles is more complicated. Moreover, the choice of proper partonic variables is frame dependent. We obtain the following kinematic equations in the hadron center of mass system:

$$M^2 = m_1^2 + m_2^2 + \xi_1\xi_2 P_1^- P_2^+ + \frac{(m_1^2 + \vec{p}_{1\perp}^2)(m_2^2 + \vec{p}_{2\perp}^2)}{\xi_1\xi_2 P_1^- P_2^+} - 2\vec{p}_{1\perp} \cdot \vec{p}_{2\perp};$$
$$x_F = \frac{\sqrt{S}}{S - M^2}\left(\xi_2 P_2^+ - \xi_1 P_1^- + \frac{(m_1^2 + \vec{p}_{1\perp}^2)}{\xi_1 P_1^-} - \frac{(m_2^2 + \vec{p}_{2\perp}^2)}{\xi_2 P_2^+}\right). \quad (33)$$

Here, we have used:

$$\xi_1 = p_1^-/P_1^-, \qquad \xi_2 = p_2^+/P_2^+, \quad (34)$$

P_1 (P_2) is the 4-momentum of the target (projectile) hadron, $p_{1,2}$ denote momenta of the annihilating quark and antiquark, M^2 is the invariant mass squared of the produced leptons. S denotes the hadron center of mass energy

squared. The Feynman variable is defined as $x_F \equiv p_z/(p_z)^{max}$, where $\vec{p}$ is the lepton pair momentum. In some works, an approximate definition for the Feynman variable is used: $x_F \approx 2p_z/\sqrt{S}$. We used the exact definition [28] that can be written in the hadron center of mass system as follows

$$x_F \equiv \frac{p_z}{(p_z)_{max}} = \frac{2p_z\sqrt{S}}{S - M^2}. \tag{35}$$

Experimentally observed Drell-Yan pairs have small M^2 compared to S, so the difference between the two definitions of x_F are small. However, in the Drell-Yan scaling limit, $M^2 \sim S$ and the difference is finite (see formula (53) in Appendix A).

One sees that the definition of ξ_2 is analogous to the DIS case, whereas the target's momentum fraction is defined as a ratio of minus-components. In some articles, alternative definitions are used, for example $\xi_1 = p_1^+/P_1^+, \xi_2 = p_2^+/P_2^+$. The choice of the definitions (34) is based on the behavior of the hadron momenta in the Drell-Yan scaling limit ($S \to \infty$). The argument is presented in Appendix A. One might prefer to do the calculations in the target rest frame, since the connection between the observables (S, M^2, x_F, p_T) on the one hand and the partonic variables (ξ_i, m_i^2, $p_{i\perp}$) on the other is simpler in this case (cf. (57) in Appendix A). However, factorization in the form (10) is not applicable in this frame of reference (for a detailed discussion see Appendix A).

We have calculated the pQCD cross section of the off-shell quark-antiquark annihilation into a pair of dileptons:

$$\frac{d\hat{\sigma}}{d\vec{p}_1'd\vec{p}_2'} = \frac{e^4 e_q^2 \left[\hat{t}^2 + \hat{u}^2 - m_1^4 - m_2^4 + \hat{s}(m_1 + m_2)^2\right]}{16\pi\epsilon_1'\epsilon_2'\hat{s}^2 N_c\sqrt{(p_1 \cdot p_2)^2 - m_1^2 m_2^2}}\delta(p_1 + p_2 - p_1' - p_2'), \tag{36}$$

where $\vec{p}_{1,2}'$ are the three-momenta of the leptons, $\epsilon_{1,2}'$ their energies, and e_q the parton charge in units of the proton charge, color factor $N_c = 3$.

The off-shell partonic cross section, differential over the Drell-Yan process observables – mass M, Feynman variable x_F, and transverse momentum p_T of the lepton pair – is:

$$\frac{d\hat{\sigma}}{dM^2 dx_F dp_T^2} = \int \frac{d\vec{p}_1'}{2\epsilon_1'}\frac{d\vec{p}_2'}{2\epsilon_2'}d\phi\, \kappa \left[\hat{t}^2 + \hat{u}^2 - m_1^4 - m_2^4 + \hat{s}(m_1 + m_2)^2\right]$$
$$\times \delta(p_1 + p_2 - p_1' - p_2')\delta(p - p_1' - p_2'); \tag{37}$$

$$\kappa = \frac{\alpha^2 e_q^2 (S - M^2)}{\sqrt{S}EM^4 8N_c\sqrt{(p_1 \cdot p_2)^2 - m_1^2 m_2^2}}. \tag{38}$$

After performing analytically the seven integrations over non-measured quantities, four δ-functions are integrated out and the remaining four preserve the correct relation between the hadronic and partonic variables (*cf.* (33)):

$$\frac{d\hat{\sigma}}{dM^2 dx_F dp_T^2} =$$

$$\kappa' \left[\frac{M^2}{8} \left(M^2 + (m_1 + m_2)^2 \right) + \frac{E^2}{6} \left(4\,\epsilon_1^2 - m_1^2 \right) - \frac{E}{3} \epsilon_1 \left(M^2 + m_1^2 - m_2^2 \right) \right]$$

$$\times \delta \left(M^2 - m_1^2 - m_2^2 - \xi_1 \xi_2 P_1^- P_2^+ - \frac{(m_1^2 + \vec{p}_{1\perp}^2)(m_2^2 + \vec{p}_{2\perp}^2)}{\xi_1 \xi_2 P_1^- P_2^+} + 2\vec{p}_{1\perp}\vec{p}_{2\perp} \right)$$

$$\times \delta \left(x_F - \frac{\sqrt{S}}{S - M^2} \left\{ \xi_2 P_2^+ - \xi_1 P_1^- + \frac{(m_1^2 + \vec{p}_{1\perp}^2)}{\xi_1 P_1^-} - \frac{(m_2^2 + \vec{p}_{2\perp}^2)}{\xi_2 P_2^+} \right\} \right)$$

$$\times \delta \left((\vec{p}_{1\perp} + \vec{p}_{2\perp})^2 - p_T^2 \right) \delta \left(E - \epsilon_1 - \epsilon_2 \right); \quad (39)$$

$$\kappa' = \frac{\alpha^2 e_q^2 E}{M^4 N_c \sqrt{(p_1 \cdot p_2)^2 - m_1^2 m_2^2}}. \tag{40}$$

In (39),

$$\epsilon_1 \equiv \frac{1}{2} \left(\xi_1 P_1^- + \frac{(m_1^2 + \vec{p}_{1\perp}^2)}{\xi_1 P_1^-} \right), \quad \epsilon_2 \equiv \frac{1}{2} \left(\xi_2 P_2^+ + \frac{(m_2^2 + \vec{p}_{2\perp}^2)}{\xi_2 P_2^+} \right).$$

Using the ansatz (10) for the case of two off-shell partons in the initial state, we obtain the hadronic cross section by integrating over the masses and transverse momenta of quark and antiquark:

$$\frac{d\sigma}{dM^2 dx_F dp_T^2} = \sum_i \int d\vec{p}_{1\perp} \int d\vec{p}_{2\perp} \int_0^\infty dm_1 \int_0^\infty dm_2 \int_0^1 d\xi_1 \int_0^1 d\xi_2 \mathrm{A}(m_1)\mathrm{A}(m_2)$$

$$\times f_i(Q^2, \xi_1, \vec{p}_{1\perp}) \bar{f}_i(Q^2, \xi_2, \vec{p}_{2\perp}) \frac{d\hat{\sigma}}{dM^2 dx_F dp_T^2}. \tag{41}$$

The integration in (41) is 8-fold, $d\hat{\sigma}$ is given by equations (39) and (40). The common parametrization for the unintegrated parton distributions is [11, 13, 29]

$$f(Q^2, \vec{p}_\perp, \xi) = f(\vec{p}_\perp) \cdot q(Q^2, \xi), \tag{42}$$

where

$$f(\vec{p}_\perp) = \frac{1}{4\pi D^2} \exp\{ -\frac{\vec{p}_\perp^2}{4D^2} \}, \tag{43}$$

and $q(Q^2, \xi)$ is the conventional parton distribution. For the latter, we have used the latest parametrization by Glück, Reya, Vogt [30]. The mean primordial transverse momentum of partons is

$$< \vec{p}_\perp^2 > = 4D^2. \tag{44}$$

The Gaussian form of $f(\vec{p}_\perp)$ allows the analytical evaluation of the integrals over $\vec{p}_{1\perp}$ and $\vec{p}_{2\perp}$. Then, we are left with a four-dimensional integral to be done numerically. In the special case of a constant spectral function width, one of the integrals over the off-shellness can be reduced to a superposition of special functions (incomplete elliptic integrals).

We compare the result of our model, in which the partons in the proton have a finite width, with the experimental data and with the cross sections obtained by two other methods (LO pQCD and the intrinsic-k_T approach).

In k_T-factorization, the formula

$$d\sigma = f(\xi_1, \vec{p}_{\perp 1}) f(\xi_2, \vec{p}_{\perp 2}) \otimes d\hat{\sigma}(\xi_1, \xi_2, \vec{p}_{\perp 1}, \vec{p}_{\perp 2}) \qquad (45)$$

is used, where $d\hat{\sigma}$ is the Born cross section for the $q\bar{q}$ annihilation into a pair of leptons, $f(\xi, \vec{p}_\perp)$ is the unintegrated parton distribution defined in (2). A proof for the k_T-factorization in the Drell-Yan process is given in the leading twist in [31, 32]. In this case, the primordial transverse momenta of the q and $\bar{q}$ have (in general, non-zero) values defined by these distributions in the same way as the usual integrated parton distributions define the light cone fractions of the parton momenta (p^+ for the projectile parton and p^- for the target parton). In [31, 32], the fourth component of the parton momentum (p^- for the projectile parton or p^+ for the target parton) is set to zero due to the following reason. For large hard scales M, the projectile parton momentum is $p_2 = (p_2^+, p_2^-, \vec{p}_{2\perp}) \sim M(1, \lambda^2, \vec{\lambda})$, where $\lambda = m_2/M$. The parameter λ is small for $M > 1$ GeV, since the parton off-shellness and transverse momentum are related to the inverse of the confinement radius and do not scale with M. There exist several parametrizations of unintegrated parton distributions $f(\xi, \vec{p}_\perp)$.

A phenomenological 'intrinsic-k_T approach' has been developed on the basis of the k_T-factorization theorem. In this model, the unintegrated distributions are taken in the form (43),(44). An additional difference from [31, 32] is that the smaller light cone component of the parton momentum is put to its on-shell value: $p_2^- = \vec{p}_{2\perp}^2/p_2^+$, which is small, but not zero. This approach is well described in the literature [11, 12, 13, 14] and proves to be very useful for the calculation of cross sections and asymmetries of different processes. It is obtained from (41) by putting all parton masses to 0 and dropping the mass integrations and spectral functions.

In the works [13, 14], the Drell-Yan process was studied in the scope of the intrinsic-k_T approach. We can obtain the partonic Drell-Yan cross section in the k_T-factorization approach (with on-shell partons) by putting $m_1^2 = m_2^2 = 0$ in (39), (40). In particular, the following kinematic relations
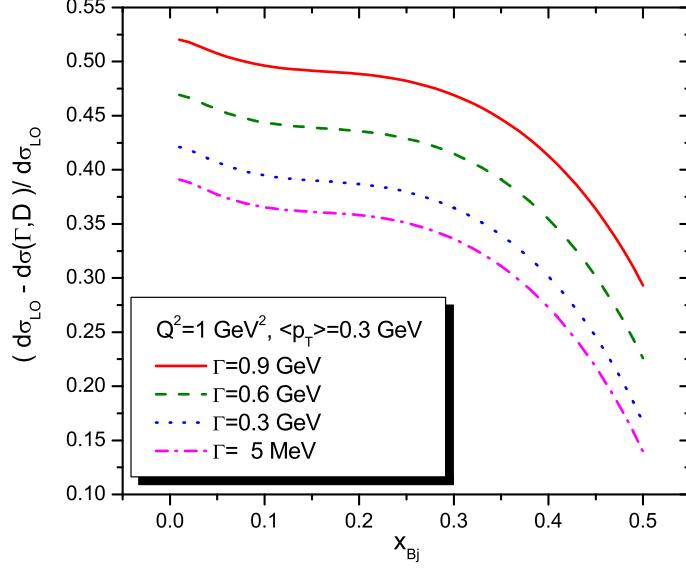
Figure 2: Relative deviation of the calculated DIS cross section from eq.(18) for the range of parton spectral function widths 5 MeV to 0.9 GeV. Mean intrinsic transverse momentum is 0.3 GeV. $Q^2 = 1$ GeV^2, $s \gg Q^2$.

are ensured by the δ-functions in this case:

$$M^2 = \xi_1 \xi_2 P_1^- P_2^+ + \frac{\vec{p}_{1\perp}^2 \vec{p}_{2\perp}^2}{\xi_1 \xi_2 P_1^- P_2^+} - 2\vec{p}_{1\perp} \cdot \vec{p}_{2\perp};$$

$$x_F = \frac{\sqrt{S}}{S - M^2} \left(\xi_2 P_2^+ - \xi_1 P_1^- + \frac{\vec{p}_{1\perp}^2}{\xi_1 P_1^-} - \frac{\vec{p}_{2\perp}^2}{\xi_2 P_2^+} \right). \tag{46}$$

The authors of [13, 14] used the parton model partonic cross section and the approximate kinematical relations (54) for simplicity. In section 3.2, we compare the cross section calculated in our model with off-shell partons to the result of the k_T-factorization approach. In order to perform such a comparison, we have calculated the Drell-Yan cross section in the intrinsic-k_T approach by using the full on-shell partonic cross section and the exact kinematics (46).
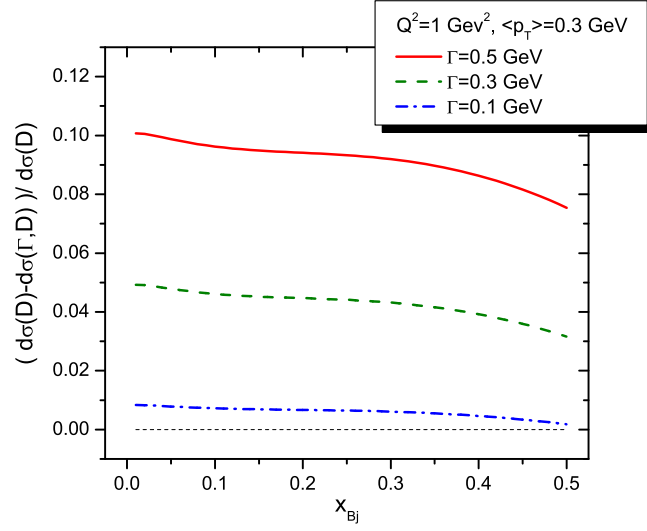
14

Figure 3: Relative deviation of the calculated DIS cross section from the result of the on-shell calculations taking into account only intrinsic transverse momentum effects. $Q^2 = 1$ GeV^2, $s \gg Q^2$.
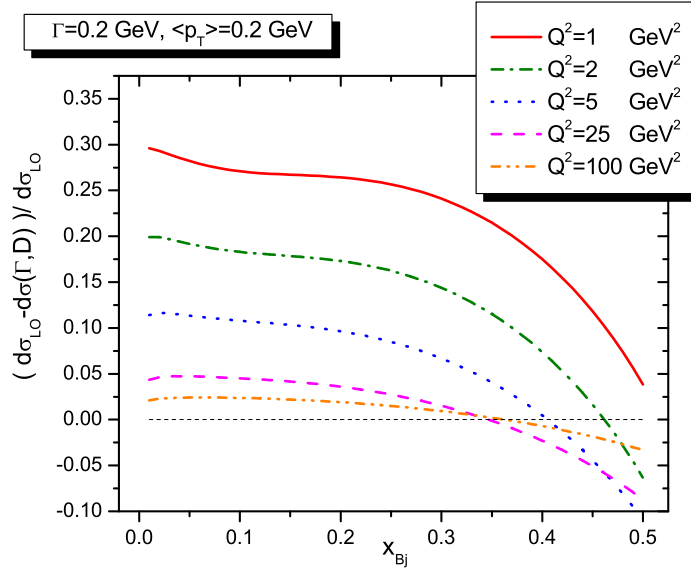

Figure 4: Relative deviation of the calculated DIS cross section from eq. (18) for different Q^2. The spectral function width is fixed to $\Gamma = 0.2$ GeV and the transverse momentum dispersion to $D = 0.1$ GeV, $s \gg Q^2$.

3 Results

3.1 DIS

The results of our calculations for the deep inelastic electron-proton scattering cross section for a range of widths as compared to the parton model (eq. (18)) are shown in fig. 2. We have found that there is a moderate effect of the initial state interaction in DIS in the region of small Bjorken x_{Bj} and low momentum transfer Q^2. The cross section deviation reaches 50% at $Q^2 = 1$ GeV^2, if the parton spectral function width and mean transverse momentum are both equal to 300 MeV. In fig. 2, one can also see that the cross section calculated in our model differs from the LO even when the parton width is negligibly small (5 MeV). This effect is due to the non-vanishing intrinsic transverse momentum.

To separate the effects of the parton off-shellness from those of the intrinsic transverse momentum, we plot the relative difference between the result of our model with off-shell partons and the calculations taking into account only the intrinsic transverse motion (fig. 3). To obtain the cross section in the latter approach, we put Γ to zero in the formulas of section 2.1 thus forcing the parton on-shell. It is seen that this difference amounts to at most 10 % of the cross section.

For values of Q^2 above 25 GeV^2, the initial state interaction in DIS gives at most a 5% deviation from the lowest order cross section (18). The Q^2-suppression of parton virtuality and intrinsic transverse momentum effects in DIS is illustrated in fig. 4. For most of the experimentally investigated values of Q^2, the ambiguity in the parton distribution function parameterizations due to the renormalization scale uncertainty is of the same order as the ISI effect in DIS.

The difference between the off-shell result and the leading order cross section at $Q^2 \geq 2$ GeV^2 is too small to be resolved by the present experiments. In the region of $Q^2 \leq 2$ GeV^2, the difference is $30 - 40$ %, which should be observable. However, in order to make a quantitative comparison to the experiment at such low Q^2 and x_{Bj}, we would have to incorporate into our model other effects, such as resonance production and diffractive scattering [33, 34, 35]. We conclude that, using the model described in the present paper, we cannot extract the value of the parton width in the nucleon from the DIS data. This is the result expected by the analogy to nuclear physics, because the DIS cross section is too inclusive. On the other hand, the DIS data do not contradict the assumption of a finite parton width in the proton.

3.2 Drell-Yan process

In contrast to the DIS case, the effect of parton off-shellness on the transverse momentum distribution of the Drell-Yan lepton pairs is substantial. In this section, we present the Drell-Yan triple differential cross section calculated by the method described in Section 2.2. We compare the result of our model, in which the partons in the proton have a finite width, with the experimental data and with the cross sections obtained in two other approaches (LO pQCD and standard k_T-factorization).

Calculations using LO pQCD and collinear factorization analogous to (1)

$$d\sigma = f(\xi_1)f(\xi_2) \otimes d\hat{\sigma}(\xi_1, \xi_2) \tag{47}$$

give a simple result for the triple differential Drell-Yan cross section (p_T-distribution of the dileptons) - a δ-function at zero p_T. This follows from the fact that the annihilating q and $\bar{q}$ in this approach are collinear with the corresponding hadrons, thus the $q\bar{q}$ pair has no transverse momentum in the hadron center of mass system. Therefore, the resulting lepton pair cannot gain any transverse momentum in this model. In contrast, the experimentally measured transverse momentum distribution of the dileptons extends to $p_T = 4$ GeV at a hard scale (the mass of the lepton pair M) as high as 8.7 GeV. Note that NLO corrections do not cure the disagreement with the data. The Drell-Yan pair p_T-distribution obtained in fixed order pQCD is divergent at $p_T = 0$. A resummation of an infinite series of diagrams is necessary to obtain a finite value for the triple differential Drell-Yan cross section at $p_T = 0$ in pQCD with on-shell partons [18]. The resummed pQCD cross section is in qualitative agreement with experiment [18].

In order to analyze the effect of a finite parton width and distinguish it from the effect of the intrinsic transverse momentum, we have performed the calculations in both the intrinsic-k_T approach and in our model allowing for off-shell partons. We used the formalism developed in Sec. 2.2 to calculate the cross section of the Drell-Yan process in the kinematics of the experiment E866 [36, 21] in the intrinsic-k_T approach and for a parton off-shellness distributed according to the Breit-Wigner spectral function (12).

We present the obtained cross sections for different values of the parameters in figures 5 and 6. We illustrate in fig. 5 that the slope of the distribution mainly depends on the dispersion of the intrinsic transverse momentum (D), which is proportional to the primordial transverse momentum of the parton (see (44)). In the limit, in which the dispersion of the intrinsic transverse momentum (D) goes to zero, the leading order result of perturbative QCD, *i.e.* a sharp peak at $p_T = 0$, is restored.
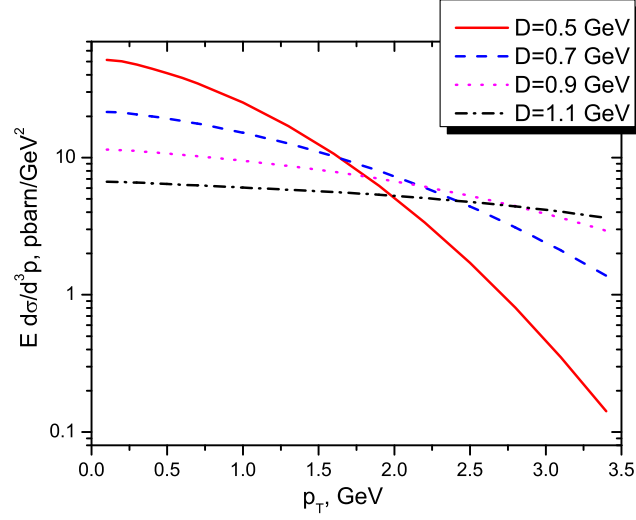
Figure 5: Calculated distribution of the Drell-Yan lepton pair's transverse momentum in the k_T-factorization approach for different values of the parton primordial transverse momentum dispersion. $M = 4$ GeV, $x_F = 0.1$, $\Gamma = 0$.
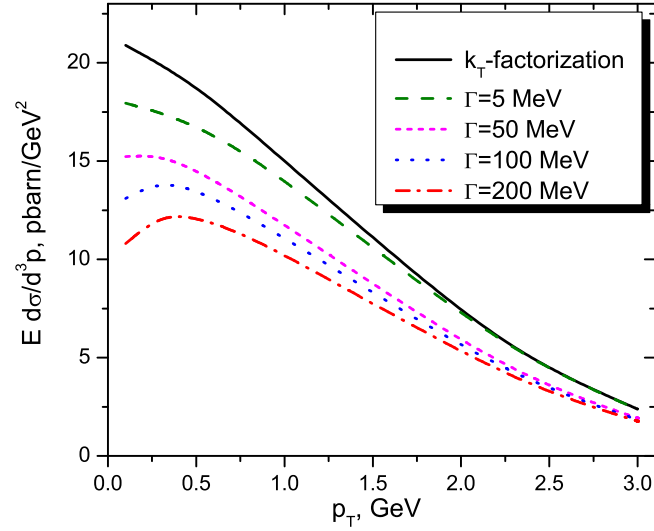

Figure 6: Calculated distribution of the Drell-Yan lepton pair's transverse momentum in our model for different values of the parton spectral function width. $M = 4$ GeV, $x_F = 0.1$, $D = 0.7$. The solid line gives the result of a calculation with $\Gamma = 0$.

18

On the other hand, the parton width variation leads to changes of the cross section magnitude and influences the behavior of the distribution in the region of low p_T (see fig. 6). One can also see in figure 6 that our model approaches the result of the standard intrinsic-k_T method as the parton width (Γ) goes to zero. At finite width, the shape of the cross section obtained in our model is different from the result of the intrinsic-k_T approach in the low p_T region. Also, the magnitude of the cross section is different. This indicates that some additional nonperturbative effects are included via a finite parton width.

In figures 7-12, calculations both in the model with off-shell partons and in the standard k_T-factorization approach are compared to the data of the Fermilab experiment E866 for the continuum dimuon production in pp collisions at 800 GeV incident energy. In this experiment, both the double differential Drell-Yan cross section $d\sigma/dM^2dx_F$ (data published in [36]) and the triple differential cross section $d\sigma/d\vec{p}$ (data published in [21]) were measured in a wide range of M and x_F ($\vec{p}$ is the lepton pair's momentum). The p_T-distribution was obtained in terms of the triple differential cross section averaged over the azimuthal angle of the lepton pair

$$\frac{d\sigma}{d\vec{p}} \equiv \frac{2}{\pi\sqrt{s}} \frac{d\sigma}{dx_F dp_T^2} = \frac{2}{\pi\sqrt{s}} \int\limits_{\text{bin}} \frac{d\sigma}{dx_F dp_T^2 dM^2} \, dM^2. \tag{48}$$

The data points were averaged in several bins in M and x_F. The x_F binning is responsible for the wiggly structures both in the data and some of our calculations.
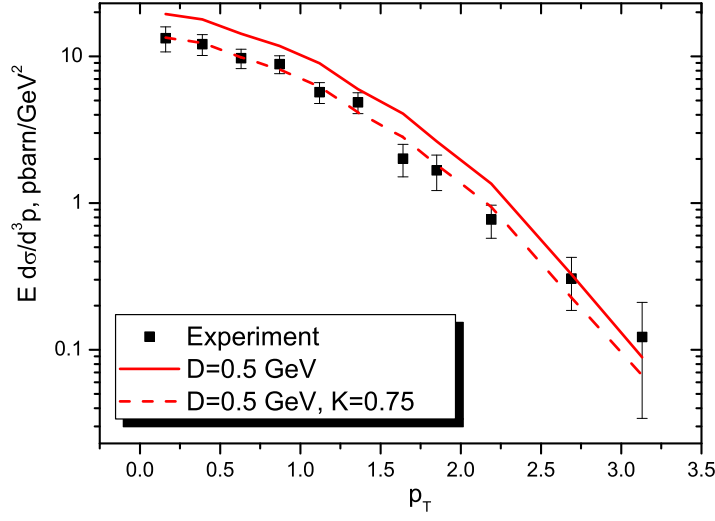
The result of the standard k_T-factorization approach is shown in figures 7 and 8 (solid line). The slope of the cross section can be reproduced by an appropriate choice of the single parameter (D) of the intrinsic transverse momentum distribution, given by (43). The optimal values for D are $500 - 600$ MeV, which correspond to

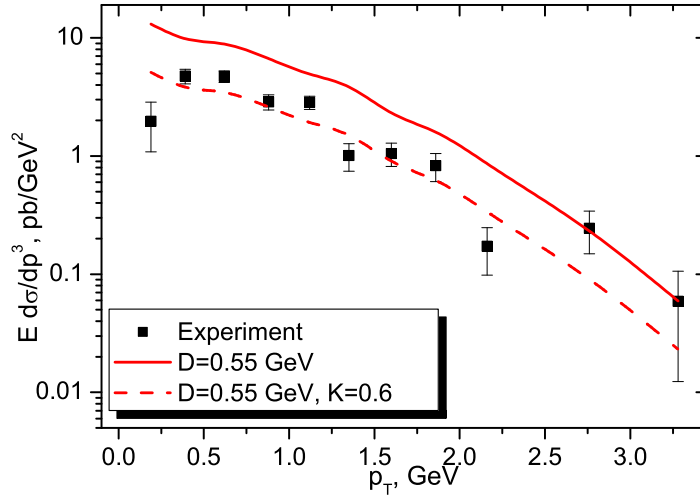$$< p_\perp^2 >^{1/2} = 1.0 - 1.2 \text{ GeV}. \tag{49}$$

A slightly smaller value for this parameter was obtained in [13, 14] from the analysis of the data of the experiment E744 on Drell-Yan cross section in pp collisions at 400 GeV incident energy:

$$< p_\perp^2 >^{1/2} = 0.8 - 1.0 \text{ GeV}. \tag{50}$$

Still, the data are overestimated by a factor of $2 - 3$, depending on the mass of the Drell-Yan pair (M). Dashed lines in figures 7 and 8 illustrate that the data can be fitted by introducing an additional overall factor (K).
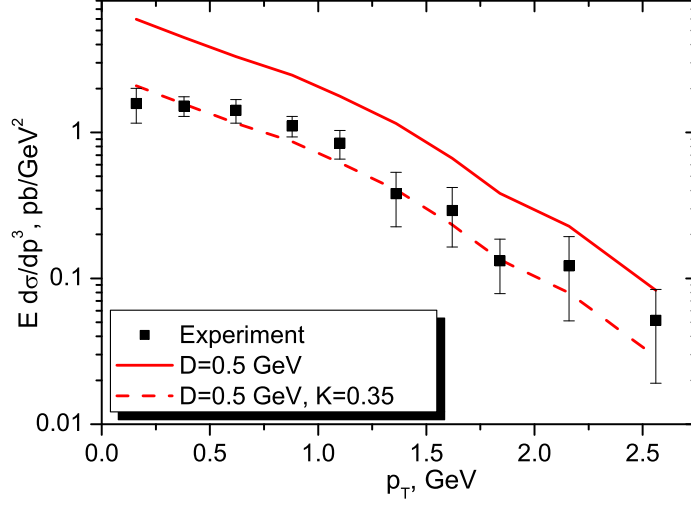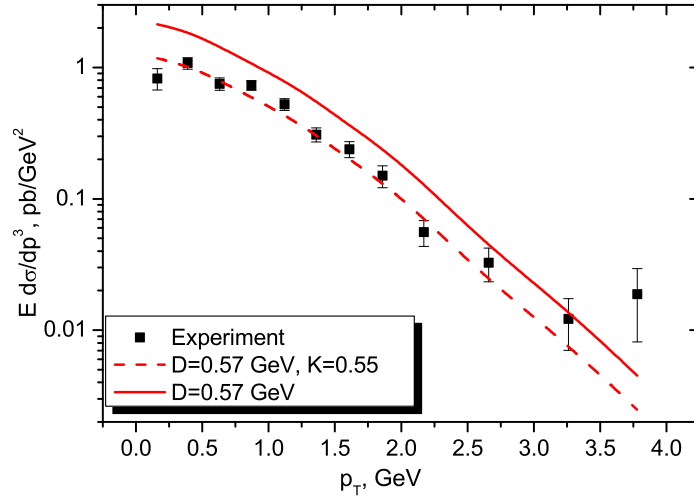
19

(a) $4.2 \leq M \leq 5.2$ GeV

(b) $5.2 \leq M \leq 6.2$ GeV

Figure 7: Drell-Yan cross section in k_T-factorization approach compared to the data for continuum dimuon production in pp collision from [21]. Varying the dispersion of intrinsic transverse momentum (D), the slope of the distribution is fitted (solid line). An additional overall K-factor is necessary to reproduce the cross section amplitude (dashed line), $-0.05 \leq x_F \leq 0.15$.

(a) $6.2 \le M \le 7.2$ GeV

(b) $7.2 \le M \le 8.7$ GeV

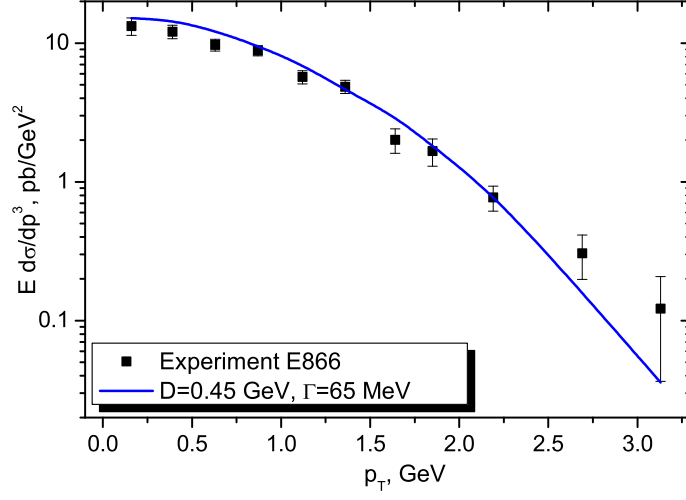Figure 8: Same as Fig. 7, but higher mass bins.

Figure 9: The Drell-Yan cross section as calculated in our model (solid line) compared to the data of the Fermilab experiment E866 for the continuum dimuon production in 800 GeV proton, $4.2 \leq M \leq 5.2$ GeV, $-0.05 \leq x_F \leq 0.15$.
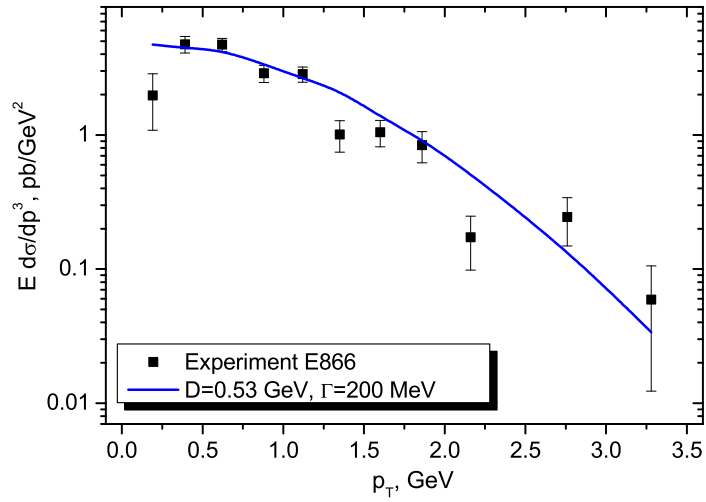

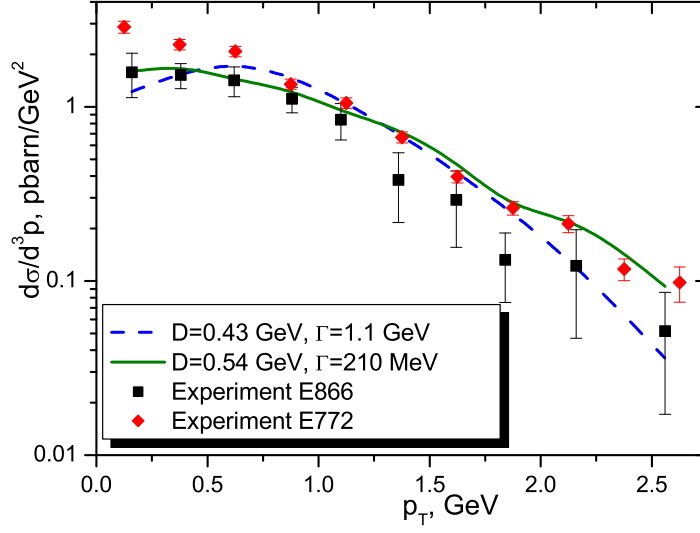Figure 10: Same as fig. 9, only for a higher mass bin: $5.2 \leq M \leq 6.2$ GeV.

Figure 11: The Drell-Yan cross section as calculated in our model compared to the data of E866 on $pp \rightarrow \mu^+\mu^- X$, $6.2 \leq M \leq 7.2$ GeV, $-0.05 \leq x_F \leq 0.15$, and to the data of E772 on $pd \rightarrow \mu^+\mu^- X$, $6 \leq M \leq 7$ GeV, $0 \leq x_F \leq 0.3$. See main text for more details about the different lines.
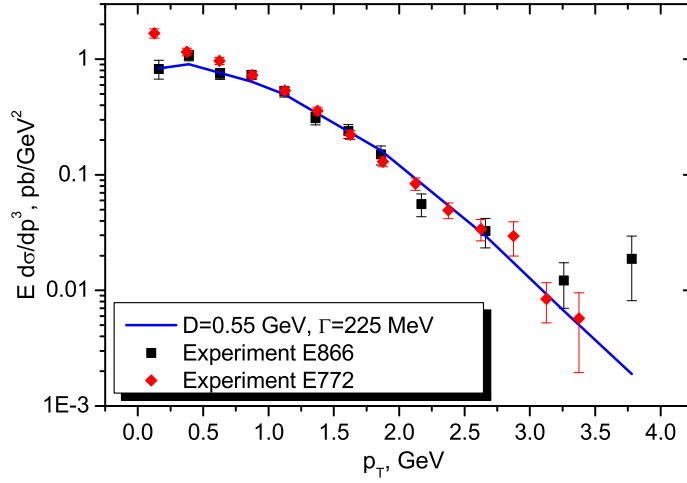

Figure 12: Same as fig. 11, only for a higher mass bin: $7.2 \leq M \leq 8.7$ GeV.

The discrepancy between the calculations and the data is larger for higher M. Thus, in the k_T-factorization approach, the magnitude of the cross section cannot be correctly reproduced. An additional overall K-factor is necessary that reflects the importance of higher order corrections to the Drell-Yan cross section.

In contrast, the calculations with a finite parton width yield not only the experimentally measured shape of the cross section but also its amplitude without any K-factor. Instead, we take care of the higher-twist and NLO effects assumed to be contained in K by introducing the physically transparent off-shellness (Γ). Note that we work in leading order of perturbative QCD concerning the processes that enter the calculation of the Drell-Yan cross section. At NLO of perturbative QCD, additional processes contribute, namely, gluon bremsstrahlung ($q\bar{q} \to l^+l^-g$), gluon Compton scattering ($gq \to l^+l^-q$ and $g\bar{q} \to l^+l^-\bar{q}$), and vertex corrections. The bremsstrahlung, along with diagrams of even higher order and with gluon exchanges between the active (anti-)quark and the spectators, contributes to the quark width. Therefore, going to higher orders of standard perturbation theory, while dressing quark lines with spectral functions, would be a double counting. In other words, we have already included part of the NLO processes by our finite width calculation. Some processes beyond the NLO are also included. On the other hand, our model can be improved by taking into account also gluon Compton scattering and vertex corrections. In this case, the gluon line should be dressed, too, and the number of model parameters increases. In the present paper, we concentrate on the effect of a finite quark width on observables and consider only the leading reaction mechanisms, *i.e.* $q\bar{q}$ annihilation for the Drell-Yan process.

The comparison of our results with the data is given in figures 9-12. The values for the average parton primordial transverse momentum

$$< p_\perp^2 >^{1/2} = 0.9 - 1.1 \text{ GeV} \tag{51}$$

are compatible with those existing in the literature (50). Allowing for off-shell partons, we eliminate the need for any K-factor. Choosing Γ in the order of 100 MeV (*cf.* table 1 for details), both the amplitude and the slope of the cross section are well reproduced.

The dependence of the optimal values for the parameters (dispersion D and width Γ) on the mass of the Drell-Yan pair was obtained by fitting experimental data within different bins of M independently. The result is presented in figures 7-12 and in table 1. Note that the varying quality of the data in different mass bins leads to large uncertainties in the extraction of the width. In table 1 we present the average values and uncertainties for

M	4.2-5.2	5.2-6.2	6.2-7.2	7.2-8.7
D	450 ± 100	530 ± 70	540*	550 ± 60
Γ	65 ± 20	200 ± 75	210*	225 ± 75

Table 1: Optimal parameters for different masses of the Drell-Yan pair, $-0.05 \leq x_F \leq 0.15$. All values are in MeV. Values denoted with stars are trend-average and not best-fit. See main text for details.

D and Γ. The latter have been obtained by analyzing the χ^2 values as a function of D and Γ. We find that the optimal Γ increases with the hard scale (the mass of the Drell-Yan pair). The dependence of Γ on M indicates that, at higher scales, partons with broader spectral functions are probed. We did not study the dependence of our parameters on x_F.

The analysis of the data in the mass bin $6.2 \leq M \leq 7.2$ GeV calls for more discussion. As shown in figure 11, the best fit (dashed line) to this data set leads to values for both parameters (D=0.43 GeV, Γ=1.1 GeV), which are not in the trend set by the fits to the other three data bins (cf. table 1). Thus, we did not trust this fit and sought for more experimental input. For $p_T \geq 1$ GeV, the data of the experiments E866 on $pp \rightarrow \mu^+\mu^- X$ and E772 [37] on $pd \rightarrow \mu^+\mu^- X$ agree very well in all the mass bins, except the one of figure 11 (see figure 12, for example). Therefore, we compared our fit (dashed line) to the experimental data on the pd cross section from E772 in approximately the same mass range (figure 11). One can see that the calculations with $D = 0.43$ GeV and $\Gamma = 1.1$ GeV (dashed line) do not reproduce the high-p_T part of the pd cross section. On the other hand, if the trend-average values from table 1 are applied ($D = 0.54$ GeV, $\Gamma = 210$ MeV, solid line in figure 11), the cross section calculated in our model both describes the E866 data on the border of experimental error bars and reproduces the pd cross section of E772 at $p_T \geq 1$ GeV.

Allowing for a finite parton width and using a single-parameter form for the parton spectral function, we account for non-perturbative effects, including the K-factor. The result of the collinear factorization and fixed order pQCD (δ-peak at $p_T = 0$) is not reached in the experiment even at masses of lepton pairs as high as $M \sim 16$ GeV. There is one area of hard scales, where the intrinsic k_T approach seems to reproduce the cross section with good accuracy: at low M the K-factor of the intrinsic-k_T approach is closer to 1. As the dilepton mass goes higher, the measured distribution is getting more sharply peaked. This suggests that the result of LO pQCD might be recovered at Drell-Yan pair masses, which are higher than those

yet observed. On the other hand, our model allowing for off-shell partons with finite width works well for all hard scales M.

4 Summary and outlook

The research presented here reveals the importance of the parton initial state interaction for the analysis of high energy processes. We have developed a formalism to study the quark structure of hadrons going further than the widely studied picture of collinear noninteracting partons. The parton off-shellness effects missed in the standard treatment were taken into account by dressing the parton lines with spectral functions and using the factorization assumption. In this way, higher twist corrections to standard pQCD were modelled.

We have calculated the cross sections of deep inelastic ep scattering and the Drell-Yan process $pp \to l^+l^-X$ in the model allowing for a finite parton width. Off-shellness effects arise from the fact that the time-like light-cone momentum of the parton (p^-) is not fixed by an on-shell condition $(p^- = p_\perp^2/p^+)$ or by a collinearity condition $(p^- = 0)$. Since the partons in the proton interact, p^- is in fact distributed with some finite width. To disentangle the off-shellness effects from the effect of the parton primordial transverse momentum, we have additionally calculated the Drell-Yan cross section in the standard intrinsic-k_T approach. The obtained cross sections in both models were compared to the data on the triple differential cross section of the process $pp \to l^+l^-X$.

We have found a moderate effect of the initial state interaction in DIS in the region of small Bjorken x_{Bj} and low momentum transfer Q^2. For a parton width of 300 MeV, the cross section increases due to the finite quark width in the proton reaches 10% at $Q^2 = 1$ GeV^2. On the other hand, the effect is Q^2-suppressed. For values of Q^2 above 10 GeV, the initial parton off-shellness generates only at most 2% of the cross section. For most of the experimentally investigated values of Q^2, the difference between the off-shell result and the leading order cross section is too small to be resolved by present experiments. We conclude that the value of the parton width in the nucleon cannot be extracted from the DIS data, because the DIS cross section is too inclusive. This is the result expected by the analogy to nuclear physics. On the other hand, the DIS data do not contradict the assumption of the finite parton width in the proton.

In contrast, we discover a substantial contribution of the parton off-shellness to the transverse momentum distribution of the high-mass virtual photons produced in high-energy hadron-hadron collisions in the whole range

of hard scales, at which the cross section has been measured. The triple differential Drell-Yan cross section is a more exclusive observable than the DIS cross section. That is why the effect of the parton off-shellness was expected to be larger in the Drell-Yan case. Our results confirm this expectation.

Although the intrinsic-k_T approach alone can reproduce the slope of the experimentally measured distribution of dileptons, an overall K-factor is necessary to fit the data. Shape *and magnitude* of the cross section are much better reproduced by a model that allows for off-shell partons. In particular, one can fit the data without a K factor. The parton width in the proton was estimated from the comparison to the data. For a mass of the Drell-Yan pair of $4.2 - 8.7$ GeV, the best fits were obtained with quark (antiquark) width of $50 - 250$ MeV and intrinsic transverse partonic momentum dispersion of $400 - 600$ MeV. This corresponds to a mean primordial transverse momentum of the parton inside a proton of $< k_T >= 0.8 - 1.2$ GeV.

Since the Drell-Yan process is expected to be one of the leading background contributions at the future high energy facilities, it is important to predict its cross section as precisely as possible. The obtained triple differential cross section of the dilepton production in pp collisions is also a necessary input for models, studying nuclear medium via high energy dileptons, produced in pA and AA collisions. To meet this demand and to consistently evaluate the ISI effects in high energy processes, we need to improve our knowledge of the parton spectral function in the nucleon. The single-parameter Breit-Wigner parametrization might be insufficient. To pin down the parton spectral function, the study of other exclusive processes will be necessary. In particular, it should be possible to reduce the sizable uncertainty in the width. We shall address this issue in the future.

5   Acknowledgements

A   Appendix

In this appendix we present the details of the Drell-Yan process description in different frames of reference. The arguments for the definitions of the partonic momentum fractions used in our calculations are given as well.

Let us consider the Drell-Yan scaling limit ($S \to \infty$). The light cone

components of hadron momenta in the center of mass system are

$$\left(P_1^{\mp}\right)^2 = \left(P_2^{\pm}\right)^2 = \frac{S}{2} - M_N^2 \pm \sqrt{\left(\frac{S}{2}\right)^2 - M_N^2 S}. \tag{52}$$

Thus, the plus-component of the projectile's momentum P_2^+ and the minus-component of the target's momentum P_1^- go to infinity $\sim \sqrt{S}$, while all the other components are negligible in the scaling limit.

With the chosen definitions of ξ_i, we get as a limit of (33):

$$M^2 = \xi_1 \xi_2 S;$$
$$x_F = \frac{\xi_2 - \xi_1}{1 - \xi_1 \xi_2}. \tag{53}$$

Applying approximate definition $x_F \approx 2p_z/\sqrt{S}$, we recover the well known parton model relations:

$$M^2 = \xi_1 \xi_2 S;$$
$$x_F = \xi_2 - \xi_1. \tag{54}$$

This means that we can use $\xi_1 = p_1^+/P_1^+$, $\xi_2 = p_2^-/P_2^-$ as the arguments of the parton distribution functions in the factorization formula for the Drell-Yan process in the center of mass system.

In contrast, hadron light cone momenta scale differently in the target rest frame:

$$P_2^{\pm} = \frac{S}{2M_N} - M_N \pm \sqrt{\left(\frac{S}{2M_N}\right)^2 - S}; \qquad P_1^{\pm} = M_N. \tag{55}$$

The motion of the projectile is again confined to the light cone. However, there is no special direction for the target parton. Therefore, one needs to parameterize the "soft" properties of the target with more general distribution functions, which depend on the 4-momentum of the parton instead of a single scalar variable ξ. These functions $W(p)$ (partonic Wigner distributions) were introduced by X. Ji in [38].

M. Sawicki and J.P. Vary [39] considered the Drell-Yan process in the target rest frame within the factorization framework. They used the analogous to DIS definitions of the both momentum fractions,

$$\xi_1 = p_1^+/P_1^+; \qquad \xi_2 = p_2^+/P_2^+; \tag{56}$$

and found scaling violation. Indeed, in the target rest frame (33) transforms to

$$M^2 = m_1^2 + m_2^2 + \frac{\xi_1 M_N}{\xi_2 P_2^+}\left(m_2^2 + \vec{p}_{2\perp}^2\right) + \frac{\xi_2 P_2^+}{\xi_1 M_N}\left(m_1^2 + \vec{p}_{1\perp}^2\right) - 2\vec{p}_{1\perp} \cdot \vec{p}_{2\perp};$$
$$x_F = \frac{1}{\omega}\left(\xi_1 M_N + \xi_2 P_2^+ - \frac{(m_1^2 + \vec{p}_{1\perp}^2)}{\xi_1 M_N} - \frac{(m_2^2 + \vec{p}_{2\perp}^2)}{\xi_2 P_2^+}\right), \tag{57}$$

28

where we used the definitions (56) and

$$\omega = \frac{\sqrt{S}}{2} \left(\frac{S}{2M_N^2} - 1 + \frac{M^2}{S} \right) / \sqrt{\frac{S}{4M_N^2} - 1}. \qquad (58)$$

Bearing in mind equations (55) and (57), we arrive at the following limiting values for M^2 and x_F:

$$M^2 = \frac{\xi_2}{\xi_1} \left(m_1^2 + \vec{p}_{1\perp}^2 \right);$$
$$x_F = 2\xi_2. \qquad (59)$$

Hence, the variables (56) do not coincide with the Bjorken variables in the Drell-Yan scaling limit.

Contrary to the statement of [39], the relations (59) are not a dynamics effect, but an artifact, caused by the use of the alternative definitions (56). At the same time, the factorization in the form (1), applying the usual $p_\perp$-dependent parton distribution functions, is not applicable in this system of reference, because the motion of the target parton is not confined to a light cone even in the high S limit.

References

[1] O. Benhar, V. R. Pandharipande, and I. Sick, JLAB-TH-98-12.

[2] M. W. Paris and V. R. Pandharipande, Phys. Lett. B **514**, 361 (2001), arXiv:nucl-th/0105076.

[3] S. J. Brodsky, P. Hoyer, N. Marchal, S. Peigne, and F. Sannino, Phys. Rev. D **65**, 114025 (2002), arXiv:hep-ph/0104291.

[4] J. Qiu and G. Sterman, Nucl. Phys. B **353** (1991) 105.

[5] P. J. Mulders and R. D. Tangerman, Nucl. Phys. B **461** (1996) 197 [Erratum-ibid. B **484** (1997) 538], arXiv:hep-ph/9510301.

[6] E. V. Shuryak and A. I. Vainshtein, Nucl. Phys. B **199** (1982) 451, E. V. Shuryak and A. I. Vainshtein, Nucl. Phys. B **201** (1982) 141.

[7] P. Hoyer, talk at the "International Conference: I.Ya. Pomeranchuk and Physics at the Turn of the Centuries", Moscow, January, 2003, arXiv:hep-ph/0307263.

[8] P. Hoyer, talk at DIS-03, St.-Petersburg, April, 2003, arXiv:hep-ph/0308019.

[9] M. Fontannaz and D. Schiff, Nucl. Phys. B **132** (1978) 457.

[10] C.-Y. Wong and H. Wang, Phys. Rev. C **58**, 376 (1998), arXiv:nucl-th/9802378.

[11] X.-N. Wang, Phys. Rev. C **61**, 064910 (2000), arXiv:nucl-th/9812021.

[12] Y. Zhang, G. Fai, G. Papp, G. Barnafoldi, and P. Levai, Phys. Rev. C **65**, 034903 (2002), arXiv:hep-ph/0109233.

[13] U. D'Alesio and F. Murgia, talk at the "IX Convegno su Problemi di Fisica Nucleare Teorica", Cortona, Oct. 9-12, 2002, arXiv:hep-ph/0211454; U. D'Alesio and F. Murgia, talk at "15th International Spin Physics Symposium", SPIN2002, Brookhaven National Laboratory, Upton (NY), Sept. 9-14, 2002, arXiv:hep-ph/0211201.

[14] U. D'Alesio and F. Murgia, Phys. Rev. D **70** 074009 (2004) arXiv:hep-ph/0408092.

[15] D. Boer, S. J. Brodsky, and D. S. Hwang, Phys. Rev. D **67**, 054003 (2003), arXiv:hep-ph/0211110.

[16] S. J. Brodsky, D. S. Hwang, and I. Schmidt, Nucl. Phys. B **642**, 344-356 (2002), arXiv:hep-ph/0206259.

[17] O. Linnyk, S. Leupold, and U. Mosel, talk at the "IV International Conference on Perspectives in Hadronic Physics", Trieste, May 12-16, 2003, published in EPJ A **19** s01, 203 (2004), arXiv:hep-ph/0308265.

[18] G. Fai, J. Qiu, and X. Zhang, Phys. Lett. B **567**, 243 (2003), arXiv:hep-ph/0303021.

[19] J. w. Qiu and X. f. Zhang, Phys. Rev. Lett. **86** 2724 (2001), arXiv:hep-ph/0012058.

[20] F. Landry, R. Brock, G. Ladinsky and C. P. Yuan, Phys. Rev. D **63** 013004 (2001), arXiv:hep-ph/9905391.

[21] J. C. Webb, PhD thesis, New Mexico State University, 2003, arXiv:hep-ex/0301031.

[22] J. C. Collins, Acta Phys. Polon. B **34**, 3103 (2003), arXiv:hep-ph/0304122.

[23] R. L. Jaffe, Lectures presented at the Los Alamos School on Quark Nuclear Physics, Los Alamos, N.Mex., Jun 10-14, 1985, Los Alamos Wrkshp. (1985) 0537, MIT-CTP-1261.

[24] O. Benhar, *preprint*, arXiv:nucl-th/0204042.

[25] O. Benhar, S. Fantoni, and G. I. Lykasov, Phys. Lett. B **502**, 69 (2001), arXiv:hep-ph/0011302.

[26] F. Froemel, S. Leupold, and U. Mosel, Phys. Rev. C **67**, 015206 (2003), arXiv:nucl-th/0111004.

[27] M. E. Peskin and D. V. Schroeder, "An Introduction To Quantum Field Theory," Addison-Wesley (1995).

[28] K. Hagiwara *et.al.*, Phys. Rev D **66**, 010001 (2002).

[29] J. Raufeisen, J. C. Peng and G. C. Nayak, Phys. Rev. D **66**, 034024 (2002), arXiv:hep-ph/0204095.

[30] M. Glück, E. Reya, and A. Vogt, Eur. Phys. J. C **5**, 461 (1998), arXiv:hep-ph/9806404.

[31] X. d. Ji, J. p. Ma and F. Yuan, *preprint*, arXiv:hep-ph/0404183.

[32] H.-N. Li, Phys. Rev. D **55**, 105 (1997), arXiv:hep-ph/9604267.

[33] M. Osipenko *et al.*, *preprint*, arXiv:hep-ex/0301033.

[34] W. Melnitchouk, AIP Conf. Proc. **588** (2001) 267, arXiv:hep-ph/0010311.

[35] A. D. Martin, M. G. Ryskin and G. Watt, Phys. Rev. D **70** (2004) 091502, arXiv:hep-ph/0406225.

[36] J. C. Webb *et al.* [NuSea Collaboration], arXiv:hep-ex/0302019.

[37] P. L. McGaughey *et al.* Phys. Rev. D **50** 3038 (1994) [Erratum-ibid. D **60** 119903 (1999)].

[38] X. Ji, Phys. Rev. Lett. **91**, 062001 (2003), arXiv:hep-ph/0304037.

[39] M. Sawicki and J. P. Vary, Phys. Rev. Lett. **71**, 1320 (1993).